Tutor/s

Dr. Alexandra Elena Plesu Popescu
Departament d'Enginyeria Química i Química Analítica

Dr. Joan Llorens Llacuna
Departament d'Enginyeria Química i Química Analítica

Grau en Enginyeria Química

Treball Final de Grau

Numerical simulation of the descendent liquid film in a vertical tube

Maria Montañes Puig

June 2020

Scientists study the world as it is;
engineers create the world that has never been.

Theodore von Karman

En primer lloc m'agradaria donar les gràcies als meus tutors i professors per haver-me ajudat a tirar endavant el meu treball final de grau sobrepassant totes les dificultats generades en aquesta època de pandèmia, des de la necessitat de la reorientació del treball fins a l'adaptació del seguiment telemàtic del projecte. Sense la seva implicació i sempre plena disponibilitat no hauria estat possible.

D'altra banda, també voldria donar les gràcies als meus pares i familiars que han contribuït a fer-me ser tal com soc avui dia i sense els quals mai hauria arribat tant lluny. Sempre són i seran les persones més importants de la meva vida tot i la distància física d'aquest últims anys. Però tampoc no em vull oblidar de les amistats forjades durant aquesta etapa de la meva vida que estic ben segura que seguiran durant anys. Ni tampoc dels amics de tota la vida amb els quals he anat obrint i tancant etapes, i tot i la distància segueixen formant part de la meva vida.

Amb aquest treball es tanca una etapa de la meva vida en la que no tan sols m'he format acadèmicament sinó que també he crescut com a persona i que és quedarà sempre en la meva memòria com una de les etapes més importants i enriquidores.

CONTENTS

SUMMARY

Nowadays, it is impossible to have doubts that technology advances have been involved on the development of the humanity, including development of chemical engineering. For example, the computer invention and their increasing calculation power gave us the opportunity to solve more easily and quickly Transport Phenomena equations. These equations, which are the basis of Computational Fluid Dynamics (CFD), had been defined by Bird many years ago (1960), but during these days their solution required an computation power out the capabilities of the computers available at that time and it depended on the ability of the human. However, now we can use them easily to simulate fluid flow and to understand it better.

In this project, the Mathematica 12.0 programming skill and the transport phenomena knowledge acquired during the degree is used to solve the mass and momentum conservation equations. With this knowledge, a recent article published by Hogxia Gao in the AIChE journal on 2018 has been reproduced. This article simulates the drop of a liquid film along a vertical tube of known dimensions. To reproduce it different models are implemented, for example a CFD model has been used to simulate the liquid film flow, by this way the film thickness and the hydrodynamics at the entry length have been predicted. The simulations are done using different liquids (distilled water / 40% water-sugar solution / 30% MEA-water solution) and different flowrates. Besides, its results have been compared with different symbolical models (two models based on Navier-Stokes equations and one based on an expression given by Bird to predict liquid film thickness along a vertical wall). and with experimental data from this reference. Hence, a total of four model has been implemented, each one of them has been applied in three mixtures to different flow rates, it means that more than 250 simulation have been done.

The results of this project compared with the available experimental data show that the implemented CFD model programmed in Mathematica 12.0 predicts quite well the film thickness but not the hydrodynamics at the entry. Moreover, they are useful to understand and get an insight about how change the film flow depending on the liquid and on the flowrate used. In

consequence, models to predict the hydrodynamics at the entry could be proposed on a future project

RESUM

En l'actualitat és impossible posar en dubte que els avanços tecnològics han contribuït al desenvolupament de la humanitat, incloïen al desenvolupament de l'enginyeria química. Un exemple d'aquests avanços va ser la invenció dels ordinadors i l'augment de la potencia de càlcul d'aquests que ens ha permès resoldre més fàcilment i ràpidament les equacions dels fenòmens de transport. Aquestes equacions, les quals són el fonament de la dinàmica de fluids computacional (CFD), van ser proposades per Bird molts anys enrere (1960). No obstant, en aquells temps la seva solució requeria un poder de càlcul superior del que disposaven els ordinador i depenia de l'habilitat humana per resoldre-les. En canvi, en l'actualitat aquestes equacions poden ser resoltes fàcilment i d'aquesta forma simular el flux de fluids per tal de poder entendre-les més fàcilment.

En aquest projecte, l'habilitat de programar amb Mathematica 12.0 i el coneixement de fenòmens de transport adquirit durant el grau han estat utilitzats per resoldre les equacions de conservació de la massa i la quantitat de moviment. D'altra banda, cal destacar que aquest projecte s'ha basat en reproduir un article publicat per Hogxia Gao a la revista AIChE durant l'any 2018. Aquest article simula el descens d'una pel·lícula al llarg d'un tub vertical de dimensions determinades. Per tal de reproduir-lo s'han implementat diferents models. Per exemple, s'ha utilitzat un model CFD per tal de simular el flux de la pel·lícula líquida i d'aquesta forma obtenir el seu gruix i la longitud de l'efecte que es produeix a l'entrada del tub. Les simulacions d'aquest flux s'han fet utilitzant tres substàncies (aigua destil·lada / una solució 40% aigua-sucre / una solució 30% aigua-MEA). A més a més, els resultats d'aquesta simulació s'han comparat amb diferents models simbòlics (dos models basats en la resolució de les equacions de Navier-Stokes i un basat amb una equació proposada per Bird per a predir el descens de una pel·lícula en una paret vertical) i amb els resultats experimentals de l'article esmentat. Per tant, aquest projecte s'han implementat un total de quatre models que han estat aplicat per estudiar la pel·lícula de tres líquids i a diferents cabals, la qual cosa ha implicat la realització de més de 250 simulacions.

Els resultats obtinguts en aquest projecte mostren que el model CFD implementat prediu de forma correcta el gruix de la pel·lícula però no la longitud de la regió d'entrada. D'altra banda, son útils per entendre com canvia el flux de la pel·lícula líquida depenent del fluid i del cabal emprat. En conseqüència, en un projecte futur es podrien proposar models per predir la longitud de l'efecte d'entrada.

1. INTRODUCTION

Nowadays, liquid film flow is in many chemical engineering processes because of its application in gas-liquid contactors such as molecular distillation towers, packed columns or tray towers. To optimize and modify these processes is important to study the mass and heat transfer on the descending liquid film. For this reason, liquid film flow has a huge influence in these studies, specifically the liquid film thickness and the entrance region length which are some of the key parameters.

In this project, an article published by Hogxia Gao (2018) in the AIChE journal has been reproduced. To do that a CFD model of a liquid film flow along a vertical tube, which dimension are describe on Figure 1, has been programmed in Mathematica 12.0. By this simulation the film thickness and entrance region length have been predicted. Moreover, the CFD model results had been compared with other models proposed in this article and with experimental data published in it. Therefore, this project can be useful to understand better liquid film flow and by this way understand better all the processes in which it is involved.

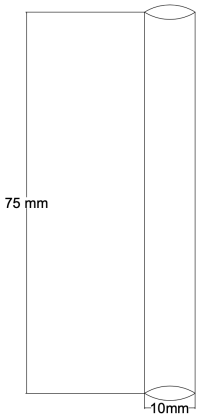

Figure 1. Tube dimensions

1.1. CFD ANALYSIS

Fluids flows is commanded by conservation laws which are expressed by partial differential equations. This conservation laws are mass conservation, momentum conservation and energy conservation.

Computational fluids dynamics (CFD) is a part of mechanical fluids that uses numerical methods and algorithms to solve fluids flows problems. An exact differential equation solution is so difficult to obtain, for this reason numerical methods are used to solve that type of equations. Specifically, these methods replace partial differential equations for algebraic equations which are solved using different software. For example, in this final project Mathematica software is used.

Using CFD a simulation of an engineering problem can be done and by this way is easier to understand it. For example, the flow, the heat transfer or the mass transfer of a process are usually simulated to understand it. Figure 2 shows an example of heat transfer CFD simulation, with this simulation the time needed to heat an adhesive located between two sheets is predicted.

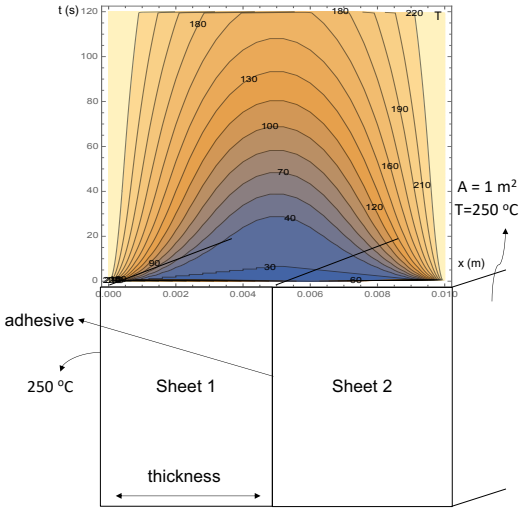

Figure 2. Heat transfer simulation (CFD)

Therefore, CFD analysis is implemented in chemical engineering field to generate qualitative or quantitative predictions of fluids flows, heat transfers or mass transfers by means of mathematical models, numerical methods and computer software.

1.2. NAVIER-STOKS EQUATION

Momentum conservation is a differential motion equation that has to be solved to obtain the velocity profiles of fluid flow. Its solution is not always easy. Inn consequence, CFD models are implemented to solve it. In this section, momentum conservation evolution is described.

. During the XVII century, Euler (Eq. 1) descried the first equations of motion which are expressed by a differential way. Motion is influenced by three forces: gravity, pressure and friction. The problem is that these equations considered gravity and pressure effects, but they did not consider viscosity which is important because it is crucial in friction forces between different materials.

$$\frac{\partial u}{\partial z} + u\,\nabla u = -\frac{\nabla \mathrm{P}}{\rho} \quad (1)$$

It was during the XIX century when Claude Navier, Augustin Cauchy, Siméon Poisson, Adhémar Barré de Saint-Venant and George Gabriel Stokes did an investigation to model these effects. As a result of it, Navier-Stokes equation was descried (Eq. 2). This differential equation is function of velocity, pressure and density as the old one, but it is also function of kinematic viscosity. Kinematic viscosity is a relation between viscosity and density.

$$\frac{\partial u}{\partial z} + u\,\nabla u = -\frac{\nabla \mathrm{P}}{\rho} + \nu\,\nabla^2 u \quad (2)$$

Navier-Stokes equation are too difficult to solve and sometimes the only way to obtain a solution is applying numerical methods. It is because they are differential equations, and these types of equations do not always have an exact solution.

To summarize, the Naiver-Stokes equation, which is also known as momentum conservation, considerate the influence of gravity, pressure and friction forces on fluids flow. Therefore, to obtain the velocity profile this equation has to be solved and, In some cases, a CFD models is necessary to do it.

1.3. LIQUD FILM FLOW

This project is based on the simulation of the drop of a liquid film along a vertical tub, in consequence understanding the liquid film flows is crucial to its development. For this reason, in this chapter liquid film flow is described. Based on some theories this flow can be divided in three parts: the uniform flow region, the entrance region and the fully developed flow region. In this section these regions are also described and a sketch of them are done on Figure 3

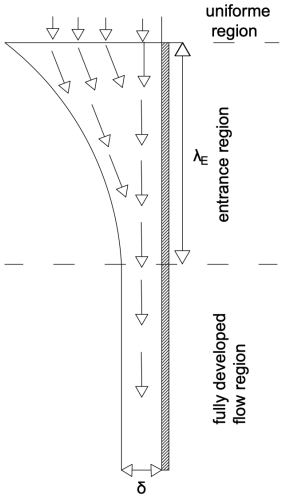

Figure 3. Liquid film flow sketch

The **uniform flow region** is located on the entrance of the tube, in this region the liquid entered to the tube at a uniform velocity but when it hits with the tube walls, a velocity profiled is formed. Along the **entrance region**, the velocity profile stabilizes before getting on the **fully developed flow region. I**n this region, the velocity profile is constant along the length.

The **entrance region** is very important because it produces a pression increase which affects the flow along the tube. The length of this effect, which is called hydrodynamic entrance length, is necessary to predict the velocity profile and the gas-liquid contact area. Moreover, is known that it can be seen as the point where the film thinness is equal to the boundary layer thickness. This length had been studied for many years by different scientists, below a summary of this studies is done.

First of all, *Anderssson (1985)* described a dilatant fluid using a semiparabolic velocity profile and a Newtonian fluid using a sinusoidal velocity profile and a third-order polynomial approach. Moreover, *Ruschak* (2000) and *Tekic (1984)* calculated the length of entrance effect supposing a semiparabolic velocity profile and *Roy (1984)* calculated it based one a third-order polynomial velocity profile. Moreover, the dimension of the hydrodynamic entrance effect of a laminar film flow had been calculated with a fourth-degree polynomial velocity profile by *Lawrence (1993)* and *Trela (1988)* related the entrance length with the initial film thickness based on a similar parabolic velocity profile. In this project, the length of the hydrodynamic entrance effect is calculated the based on the stabilization of the film thickness, which is one of the key parameters because it is needed to predict the entry region length and it also define the film mass transfer capacity.

The **film thickness** has also been studied for many years for example *Nusselt (1916),* who was the first to propose equations for the film flow along a vertical tube, calculated it on laminar flow but finally his theory was wrong because it did not predict the thickness correctly. Then, Kapitsa (1948) predicted a model for calculating the film thickness on a plate, but it did not work on the turbulent flow and *Bird (1960)* gave an equation, which become the most common, to predict the film thickness on a vertical plate. Furthermore, *Grigoreva (1977)* and *Grossman (1983)* presented some equations to predict the film thickness along a vertical tube but *Min (2011)* demonstrated that these equations were inconsistent. Moreover*, Hassan (1967)* gave a relation between the film thickness and the distance travelled by the liquid flow and *Murty (1973)* analysed the film thickness along an inclined wall.

Besides during years methods to measure experimentally the film thickness have been developed. They could be divided in two types: direct methods for example measurements with micrometre and indirect methods for instance measurements using radioactive trace or shadow photographs.

In summary, liquid film flow has been studied for many years by different scientist. According their studies it could be divided in three parts. By the other hand, the entry region length and the film thickness are the liquid film flow key parameters because their influence on the liquid film mass transfer capacity.

1.4. LIQUIDS PROPERTIES

Some liquid properties have a huge influence on film flow. For example, viscosity and density influence the liquid film profile, as momentum conservation equation shows, and surface tension is associated to the entry region length. Due to this influence, in this projected different liquid are used to simulate the liquid film flown along the tube. During this section the liquids which have been used and their properties are described.

The liquids that have been chosen are distilled water, a 40% water-sugar solution and a 30% water- MEA solution. The film flow is simulated under atmospheric pressure conditions at temperature of twenty-five Celsius degrees. Properties of these substances under these pressure and temperature conditions are Table 1, consulted on Álvarez (2006), Vázquez (1997) and Amundsen (2009) studies. This table shows that all of them have a similar density but a different viscosity so by this way how viscosity influenced on liquid film flow is studied.

*T*able 1. Properties of fluids at 298.15K and 101.325 Pa

Fluid	$\boldsymbol{\rho}\ (\mathbf{kg}\cdot\ \mathbf{m^{-3}})$	$\boldsymbol{\mu}\ (\mathbf{mPa}\cdot\mathbf{s})$	$\boldsymbol{\sigma}\ (\mathbf{mN}\cdot\ \mathbf{m^{-1}})$
Distilled water	997.1	0.89	72.01
40%wt sugar solution	1177.0	6.16	74.90
30%wt MEA solutions	1010.6	2.48	60.41

To sum up water, 40% water-sugar solution and 30% water-MEA solution are the liquids that have been selected to simulate the liquid film flow along the vertical tub. Their properties, which are describe on Table 1, defined the velocity profile, the film thickness and the entry region length.

2. OBJECTIVES

The main purpose of this project is to reproduce an article published recently by AIChE (2018). To achieve this some objectives are fixed:

- Learn more about liquid film flow.
- Modelling a descendent liquid film on a vertical tube by CFD methods.
- Use Mathematica 12.0 to simulate a descendent liquid film width on a vertical tube.
- Use Mathematica to solve Navier-Stokes equations
- Determine the influence of the number of the discretization length intervals on the results of the CFD model. Concretely, its influence on film thickness and on hydrodynamics entrance length.
- Compare different models and experimental data published on the AIChE article (2018) with the simulation results. By this way the validity of the CFD model could be checked
- Check the influence of liquid flowrate on the film thickness and on the hydrodynamics entrance length.
- Check the influence of the Reynolds number on the dimensionless hydrodynamics entrance length obtained by CFD model
- Check the influence of the liquid on the CFD model.
- Show the evolution of the liquid film thickness along the vertical tube depending on the liquid used and the flow rate.

3. MATERIAL AND MODEL

This section consists on the description of the material and the models applied in this project. Besides, how the literature experimental data had been obtained is also described.

All the models considerate that the drop of the liquid film is because of gravity effects, it means that there is not a significant increment of pressure along the tube longitude. Therefore, and because the temperature is constant along it, it is considerate that the liquid properties are constant along the tube.

3.1. MATERIAL

In this study, a computer software is used to do a CFD simulation and to solve Navier-Stokes equations of the liquid film flow, this software is called Mathematica. Mathematica is a program designed by Stephen Wolfram in 1988. It uses the Wolfram Language which is a programming language developed by Wolfram Research.

Specifically, the Students 12.0.0. Mac OS X version is used. It is executed in a MacBook Pro 2019 with a 14 GHz Intel Core i5 processor. To summarizes, Mathematica 12.0 is utilized to simulate the liquid film flow along the vertical tube.

3.2. CFD MODEL

The computational fluids dynamics (CFD) models usually use numerical methods and algorithms to solve problems about fluids flow that couldn't be solve with Reynolds equations. In this case, CFD is used to predict the film thickness and the hydrodynamic entrance length with Mathematica. The proposed model utilized to predict the velocity profile of a descendent liquid film is based on the subject Transports Phenomena of the Chemical Engineering degree of the University of Barcelona by J.Llorens (2019). The Mathematica code is in Appendix 1: CFD model program. This model is valid for laminar flow, which experimentally is limited by Reynolds Number

under 600, because the turbulence is not considerate. During this section model is described, including the space meshing, the equations discretization and the resolution process.

3.2.1. MESHING

CFD models are based on the discretization of the space, this could be a three-dimension (3D) mesh or a two-dimension (2D) mesh, which could be applied in different geometries.

In this study, the liquid film flows along a vertical tube (Figure 4) therefore a 2D mesh applied in a cylindrical geometry is used. Specifically, space is divided in radial direction and in axial ones. The number of radius and length intervals are not trivial because they are related on the results exactitude, hence before doing rigorous simulations the influence of radius and length intervals have to be studied.

In conclusion, the CFD model implemented to simulate liquid film flow along a vertical tub is based on a 2D mesh along the film radius and the tube length.

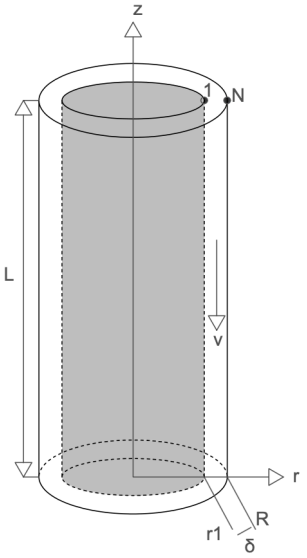

Figure 4. Sketch of liquid film flow along a vertical tube

3.2.2. MOMENTUM CONSERVATION DISCRETIZATION

To obtain the film thickness and the hydrodynamic entrance length is necessary to know the velocity profile, which is predicted using a method based on the discretization of the momentum conservation (Eq. 3). This equation is obtained assuming that liquid constant density and liquid constant viscosity.

$$r \cdot \rho \cdot u[r,z] \cdot \frac{\partial u[r,z]}{\partial z} = \frac{\partial}{\partial r} \cdot r \cdot \mu \cdot \frac{\partial u[r,z]}{\partial r} + r \cdot \rho \cdot g \quad (3)$$

The momentum conservation could be expressed by dimensionless numbers (Eq.4, Eq.5, Eq.6 and Eq.7) with are respectively the radius, the length, the film thickness and the rate.

$$r^* = \frac{r}{R} \quad (4)$$

$$z^* = \frac{z}{R} \quad (5)$$

$$\delta^* = \frac{\delta}{R} \quad (6)$$

$$u^* = \frac{u}{\frac{Q}{\pi R^2}} \quad (7)$$

Using these dimensionless number, the Reynolds Number (Eq.8) and the Froude Number (Eq.9), the momentum conservation could be redefined (Eq.10).

$$Re = \frac{\frac{Q}{\pi R^2} \cdot R \cdot \rho}{\mu} \quad (8)$$

$$Fr = \frac{\left(\frac{Q}{\pi R^2}\right)}{\sqrt{R \cdot g}} \quad (9)$$

$$r^* \cdot u^*[r,z] \cdot \frac{\partial u^*[r,z]}{\partial z^*} = \frac{\partial}{\partial r^*} \cdot \left(\frac{r^*}{Re}\right) \cdot \frac{\partial u^*[r,z]}{\partial r^*} + \frac{r^*}{Fr} \quad (10)$$

To discretize that equation Integration Over Control Volume (IOCV) is used implicit calculation method is used. According to this method the new node depends on one previous value and two adjacent values. To understand it better Figure 5 shows a sketch of this method.

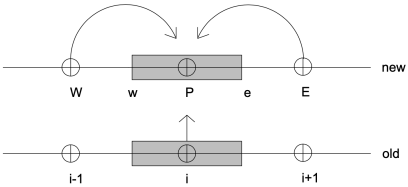

Figure 5. Sketch of implicit method

By the other side, the IOCV integration method consist in integrate separately the three parts of the differential equation (Eq.11, Eq.12, Eq.13 and Eq.14).

Part 1

$$\int_{z-\Delta z}^{z}\int_{w}^{e} \frac{\partial}{\partial r^*} \cdot \frac{r^*}{Re} \cdot \frac{\partial u^*[r,z]}{\partial r^*} \cdot dr^* \cdot dz^* = \left[\left(\frac{r^*}{Re} \cdot \frac{\partial u^*[r,z]}{\partial r^*}\right)_{i+1/2} - \left(\frac{r^*}{Re} \cdot \frac{\partial u^*[r,z]}{\partial r^*}\right)_{i-1/2}\right] \Delta z^* \quad (11)$$

$$\int_{z-\Delta z}^{z}\int_{w}^{e} \frac{\partial}{\partial r^*} \cdot \frac{r^*}{Re} \cdot \frac{\partial u[r,z]}{\partial r^*} \cdot dr^* \cdot dz^* = [AE({u_{i+1}}^* - {u_i}^*) - AW({u_i}^* - {u_{l-1}}^*)]\,\Delta z^* \quad (12)$$

Part 2

$$\int_{z-\Delta z}^{z}\int_{w}^{e} \frac{r^*}{Fr} \cdot \cdot\, dr^* \cdot dz^* = \frac{({r_{i+1}}^{*2} + {r_{i-1}}^{*2})}{4 \cdot Fr^2} \cdot \Delta z^* \quad (13)$$

Part 3

$$\int_w^e \int_{z-\Delta z}^{z} r^* \cdot v^*[r,z] \cdot \frac{\partial {v_z}^*[r,z]}{\partial z^*} \approx v_{i,z^*-\Delta z^*} \cdot \left(v_{i,z^*} - v_{i,z^*-\Delta z^*}\right) \cdot \frac{\left({r_{i+1}}^{*2} + {r_{i-1}}^{*2}\right)}{4} \quad (14)$$

Applying the general equation of implicit method (Eq. 15), velocity profile could be calculated using the flowing expressions (Eq.16, Eq.17, Eq.18, Eq.19, Eq.20, Eq.21 and Eq.22).

$$[Sp_i + AP_i] \cdot {u_i}^* = AW_i \cdot u_{i-1}^* + AE_i \cdot u_{i+1}^* + Su_i \quad (15)$$

Where:

$$AE_i = \frac{\left({r_i}^* + {r_{i+1}}^*\right)}{2 \cdot Re \cdot \Delta z^*} \quad (16)$$

$$AW_i = \frac{\left({r_i}^* + {r_{i-1}}^*\right)}{2 \cdot Re \cdot \Delta z^*} \quad (17)$$

$$AP_i = AE_i + AW_i \quad (18)$$

$$u_i^* = u_{i,z^*} \quad (19)$$

$$u_i^{o*} = u_{i,z^*-\Delta z^*} \quad (20)$$

$$Sp_i = \frac{\left({r_{i+1}}^{*2} + {r_{i-1}}^{*2}\right)}{4 \cdot \Delta z^*} \cdot \ u_i^{o*} \quad (21)$$

$$Su_i = \frac{\left({r_{i+1}}^{*2} + {r_{i-1}}^{*2}\right)}{4} \cdot \left(\frac{u_i^{o*2}}{\Delta z^*} + \frac{1}{Fr^2}\right) \quad (22)$$

However, these equations are not enough to obtain the velocity profile because the film thickness is not constant along the length of the cylinder. Concretely, it affects to the meshing because total radius, which has to be divided in intervals, is not constant along the tube length. Therefor the radial position function (Eq.23 and Eq.24) depends on the axial position.

$$r[z,i] = (R - \delta[z]) + (i-1)\Delta r \quad (23)$$

$$r^*[z,i] = (1 - \delta^*[z]) + (i-1)\Delta r^* \quad (24)$$

Hence, to obtain the velocity profile is needed to create an iterative process to solve at the same time how velocity changes along radius and which is the film thickness in each length division staring with an assuming value of film thickness. This process is founded on volumetric flow (Eq.25) conservation assuming constant density and dimensionless numbers (Eq.26)

$$Q = \sum_{i=2}^{N} \pi \left(r_i^2 - r_{i-1}^2\right) \cdot \frac{u_i + u_{i-1}}{2} \quad (25)$$

$$Q^* = \frac{Q}{V \cdot \pi \cdot R^2} = \sum_{i=2}^{N} \pi \left(r_i^{*2} - r_{i-1}^{*2}\right) \cdot \frac{u_i^* + u_{i-1}^*}{2} = 1. \quad (26)$$

Summarizing to obtain the velocity profile the momentum conservation discretization is done. But an iterative process is needed to solve at the same time the velocity profile and the film thickness.

3.2.3. RESOLUTION PROCESS

As it is said on the previous section an iterative process is needed to obtain the velocity profile this process is explained on this section. Figure 6 shows a schema of this process.

First of all, to start the resolution process is needed to enter numerical data, which are the entrance variables of CFD model. These numerical data include the properties of the fluids used (Table 1), the dimension of the cylinder (Figure 1) and a flow rate, which changes depending on the simulation.

Then it is crucial to check if there is a laminar flow with the Reynolds number because in the case of not being in this type of flow the model is not valid. Next step is doing the space division or meshing, which is done along radius and length. As it is said before this division is done using a determinate radius interval and a determinate length interval. To choose the number of length intervals a simulation of how the film thickness and the entry region length change with numbers of these intervals has been done. The dimensionless increments of radius and of length are defined on equations 27 and 28.

$$\Delta z^* = \frac{L^*}{nz} \quad (27)$$

$$\Delta r^* = \frac{\delta^*[z]}{nr} \quad (28)$$

Furthermore, before entering the radial position function is necessary to assume that dimensionless film thickness at the entrance of the cylinder (z=0) is one because the liquid film on this region fills all the cylinder section (all the radius).

After that, an assuming a value of dimensionless film thickness is required, for example in this project simulations it is 0,01. It is that moment when radius equation (Eq.23) is needed.

Another important step is defining the initial and the boundary conditions of the velocity (Table 2.) The initial condition is that at the entrance of the cylinder dimensionless velocity value is one because the film fill all the cylinder section. One the other hand, two boundary conditions are defined: the velocity on the wall is zero and on the internal part of the film is maximum. The first boundary conduction is a type one condition because value of velocity on the wall is known and the other one is a type two because it is known that velocity gradient is zero at that point.

Table 2. Initial and boundary conditions of velocity on the CFD model

Initial condition	Boundary conditions	
$u^*[0] = 1$	$u^*_{NN}[z] = 0$	$\frac{\partial u^*_1[z]}{\partial z} = 0$

Then discretization is applied on the geometry, specifically it is applied on the radial direction of one length interval. Using these equations, a solver is done to know the value of speed in every radius point and using that values liquid flowrate is obtained. When the flowrate is known, it is when the volumetric flow conservation is checked. If real value is equal calculated value, the assuming film thickness value is the film thickness of this length interval and it is time to redo the process but along another length interval. If it is not equal, the assuming film thinness value has to be changed so a new velocity profile and liquid flowrate are calculated. The new assuming film thickness value could be calculated using the dimensionless flowrate obtained (Eq.29). Repeating this process in every length point, film thickness along the tube and velocity profile are obtained.

$$\delta_{NEW}[z] = \delta_{OLD}[z] \cdot \sqrt{\frac{1}{Q}} \quad (29)$$

Finally, when film thickness is known along the tube the hydrodynamic entrance length is calculated. To do that the number of dimensionless length intervals where film thickness is not constant are counted.

To sum up an iterative process is done to obtain the velocity profile, film thickness and entry region length.

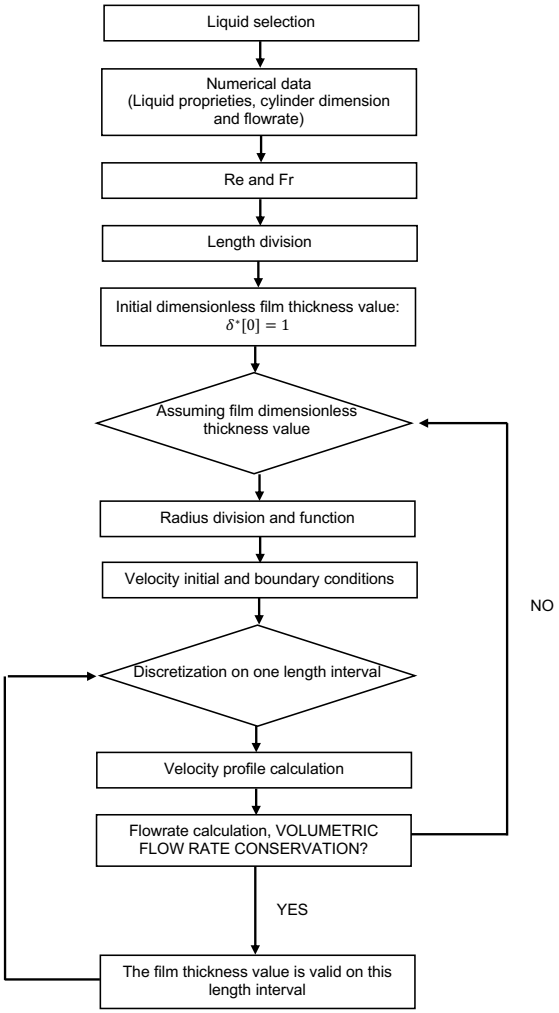

Figure 6: CFD model resolution process

3.3. NAVIER-STOKES MATHEMATICA MODEL

Another model used in this project is based on the resolution of Navier-Stokes equation using Mathematica 12.0 to obtain the film thickness. The Mathematica code is in Appendix 2: Navier-Stokes Mathematica model program,

First of all, it is important to define a velocity on the z axis, which change with the value of the radial coordinate. Then the mass and momentum conservation (Eq.30 and Eq.31) are solved and as a result four differential equations are obtained. Thre results of them are: three zeros and an equation (Eq.32), which is used to obtain the velocity profile. One of the zeros is the result of mass conservation, this result means that mass conservations is fulfilled.

$$\nabla \cdot \vec{u} = 0 \quad (30)$$

$$\frac{\partial}{\partial t}\rho\vec{u} = -\left[\nabla \cdot \rho\overrightarrow{\vec{u}\vec{u}}\right] - \left[\nabla \cdot \vec{\vec{\Pi}}\right] + \rho\vec{g} \quad (31)$$

$$-g\,\rho + \frac{\mu\, u'[r]}{r} + \mu\, u''[r] = 0 \quad (32)$$

To solve this equation two boundary conditions are needed. The first one is the velocity value on the wall, which is zero (Eq.33), and the second one is obtained from the shear stress on the wall. It can be calculated form the force balance (Eq.34) and from Newton's law (Eq.35). By this way the second boundary condition is obtained.

$$u[R] = 0 \quad (33)$$

$$\rho\, g\, L\, \pi\, (R^2 - {r_1}^2) = \tau_w\, 2\, \pi\, L\, r_1 \quad (34)$$

$$\tau = -\mu\, \vec{\dot{\gamma}} \quad (35)$$

Hence, applying a solver to the velocity differential equations and defining the boundary conditions the velocity profile equation (Eq 36.) is obtained. To obtain film thickness the liquid flow rate expression should be known. However, Mathematica 12.0 version cannot obtain liquid flow rate expression from the integration of the velocity profile between the internal radius (r1) and external radius (R), therefore an alternative way is needed. This alterative way consists in calculating the liquid flow rate numerically. Finally, internal radius is obtained using interpolation methods, by this ways the film thickness in a determinate flow rate is predicted. .

$$u[r] = \frac{g\,\rho\left(R^2 - r^2 + 2(R^2 - 2\,r_1{}^2)\log[R] - 2(R^2 - 2\,r_1{}^2)\log[r]\right)}{4\,\mu} \quad (36)$$

Summarizing a Mathematica code has been programmed to obtain the film thickness from Navier-Stokes equation resolution.

3.4. NAVIER-STOKES SIMPLIFIED MODEL

The Naiver-Stokes equation solution is not easy to get. In consequence Hogxia Gao *(2018) proposed a* simplified Navier-Stokes equation of motion for laminar flow along a vertical cylinder (Eq.37). A general solution of this equation could be easily obtained (Eq.38) and a boundary condition (Eq.39) could be used to obtain a more concrete solution (Eq.40)

$$\frac{1}{r}\frac{d}{dr}\left(r\,\frac{du}{dr}\right) = -\,\rho\,g. \quad (37)$$

$$\mu\,\frac{du}{dr} = -\frac{1}{2}\,\rho\,g\,r + \frac{c}{r} \quad (38)$$

$$u[R] = 0 \quad (39)$$

$$u = \frac{1}{4}\,\frac{\rho\,g}{\mu}\,(R^2 - r^2) + \frac{c}{\mu}\,ln\left(\frac{r}{R}\right) \quad (40)$$

Moreover, from equation 40 and Newton's law (Eq.35) the shear stress can be defined (Eq.41), as well as using force balance (Eq.42). From these expressions the constant of equation 40 can be obtained (Eqs43.)

$$\tau_w = -\frac{1}{2}\,\rho\, g\, R + \frac{c}{R} \quad (41)$$

$$\tau_w(2\,\pi\, R\, L) = \rho\, g\, \pi\, L\, (R + \delta)^2 - R^2) \quad (42)$$

$$c = \frac{1}{2}\,\rho\, g\, (R + \delta)^2 \quad (43)$$

As a result of this, velocity profile could be defined (Eq.44). Besides, to get the volumetric flowrate expression (Eq.48) velocity profile is expressed using dimensionless numbers (Eq.45, Eq.46. and Eq.47). Finally, using volumetric flow rate expression, film thickness could be predicted.

$$u = \frac{\rho\, g}{4\,\mu}\ (R^2 - r^2) + \frac{\rho\, g}{2\,\mu}(R + \delta)^2 \ln\left(\frac{r}{R}\right) \quad (44)$$

$$\phi = \frac{r}{R} \quad (45)$$

$$\alpha = \frac{\delta}{R} \quad (46)$$

$$U = \frac{\rho\, g\, R^2}{4\,\mu}\ [2\,(1+\alpha)\ln(\phi) + 1 - \phi^2] \quad (47)$$

$$Q = \frac{\pi\,\rho\, g\, R^4}{8\,\mu}|4(1+\alpha)^4\ \ln(1+\alpha) - \alpha(2+\alpha)(2+6\alpha+3\alpha^2)| \quad (48)$$

In conclusion, according Hogxia Gao (2018) Navier-Stokes equation could be simplified to obtain the film thickness of a liquid film flow.

3.5. BIRD MODEL

Bird (1960) gave a relation to calculate the liquid film thickness along a vertical wall (Eq.49). According Hogxia Gao (2018) this relation could be readapted to a vertical cylinder assuming that the width of the wall is equal to the circumference of the vertical cylinder (Eq.50).

$$\delta = \sqrt[3]{\frac{3\,\mu\,Q}{\rho\,g\,W}} \quad (49)$$

$$\delta = \sqrt[3]{\frac{3\,\mu\,Q}{2\,\rho\,g\,\pi\,R}} \quad (50)$$

In conclusion, an equation gave by Bird (1960) have been readapted to a vertical cylinder.

3.6. EXPERIMENTAL DATA

Hogxia Gao *(2018)* proposed an experimental apparatus to size the internal film thickness along a tube. A vertical polished stainless-steel vertical cylinder (Figure 7) was used for experimental test and a high-speed camera was used to obtain the film thickness. These results are used in this project as a way to check the CFD model.

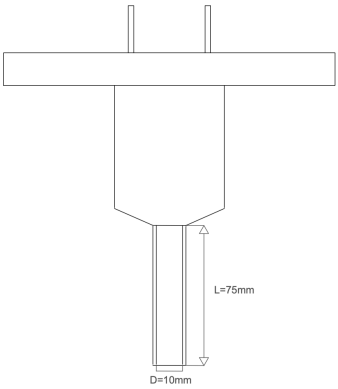

Figure 7. Sketch of experimental apparatus

4. RESULTS AND DISCUSSION

The main propose of this project is reproduce a study of liquid laminar film flow along a vertical tube published in AIChE journal recently. A CFD model have been programmed in Mathematica 12.0 to reach this propose and by this way check its validity. The results are structured in five blocks:

1. Simulations of the liquid film flow using water to check the influence of length intervals number on the CFD model.
2. Simulations of the liquid film flow using different solutions to check the influence of the flowrate on the film thickness.
3. A detailed study of the results of the CFD model entry length and the influence of the Reynolds number on it.
4. Simulations of two flowrates of the three solutions to check the effect of the liquid properties on the CFD model.
5. Sketches of different liquids film flown along the tube.

4.1. INFLUENCE OF LENGHT INTERVALS NUMBER ON CFD MODEL

To decide the number of length intervals used in the CFD model, a study of how the film thickness and the length of entrance region change depending on the number of length intervals have been done.

The study has been done using 49 radius intervals and 54.25 mL/min of distillate water to simulate the liquid film flow. The number of length intervals has been changed in every simulation by this way its influence on the film thickness and the entry region length has been checked.

The results are reflected on Figure 8, which shows how the film thickness changes with the number of length intervals, and Figure 9, which shows how changes the entry region length changes with the number of length intervals.

These figures show that number of length intervals do not affect the film thickness. In spite of this, the length of entrance region is affected if the number of intervals is too small. Besides, these simulations show that the computational time increase significantly with length intervals. In consequence, the mesh is done with 300 length intervals and 49 radius intervals.

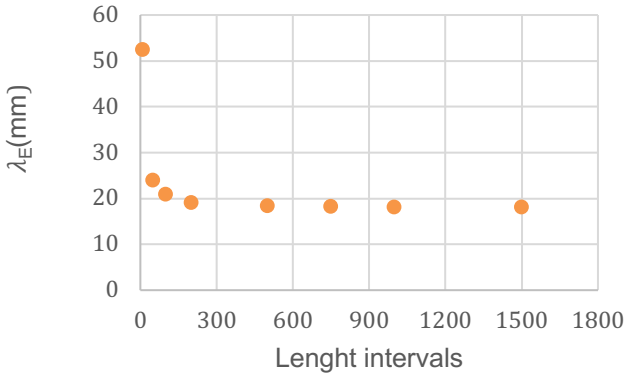

Figure 8.Influence of length intervals number on film thickness

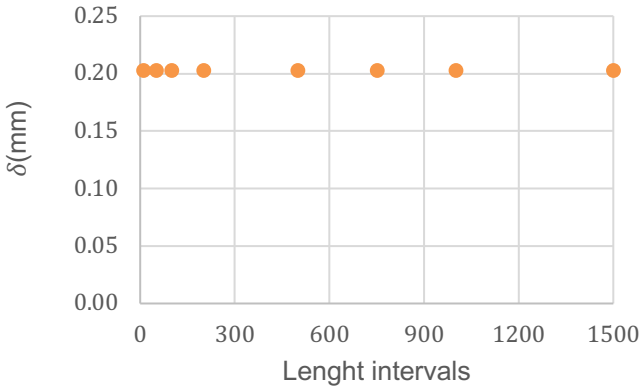

Figure 9. Influence of length intervals number on film thickness

4.2. INFLUENCE OF FLOWRATE

Different liquids are used to study how the liquid flowrate influence on the liquid film thickness and on the hydrodynamics entry length values predicted with the different models and the experimental data. It necessary to consider that these liquids have a similar density, but a different viscosity.

Moreover, comparison between the models results, including symbolical and numerical ones, and numerical data are done. They are based on experimental data published by Hogxia Gao (2018) (Appendix 3: Table 1, Table 4 and Table 7), the results of the CFD simulation ((Appendix 3: Table 2, Table 5 and Table 8) , the Navier-Stokes simplified model expression (Eq48.), the Bird model equation (Eq. 50) and the Navier-Stokes Mathematica model results ((Appendix 3: Table 3, Table 6 and Table 9). By this way, the validity of the CFD model is cheeked. The results of this section are dived in three parts:

1. Distilled water results
2. 40 % water-sugar solution results
3. 30 % water-MEA solution results

4.2.1. DISTILLED WATER

The influence of the flowrate on water film thickness and on the entry region length are show on Figure 11 and Figure 10. The first one shows a comparison of how the different models film thicknesses results and experimental data film thicknesses are influence by the flowrate. By the other side, the second figure shows a comparison of how CFD model entry region length and experimental data entrance region length are influence by the flowrate.

The results of film thicknesses (Figure 11) show that it increases with the liquid flow rate in all the data. Moreover, there is not a big difference between models and experimental date in that case, but the results of Naiver-Stokes Mathematica model differ from the others. In spite of not being a big difference between models, results show that the models are much similar to experimental data in lowers flow rates.

By the other hand, entrance effect lengths obtained with CFD model has a significant difference between experimental data (Figure 10). It may be because to simulate this process is assumed that the film on the entrances fill all the cylinder radius. Moreover, these results show

that the hydrodynamic effect length is influenced by the flow rate, concretely it increases with the liquid flow rate but experimentally it is nearly constant.

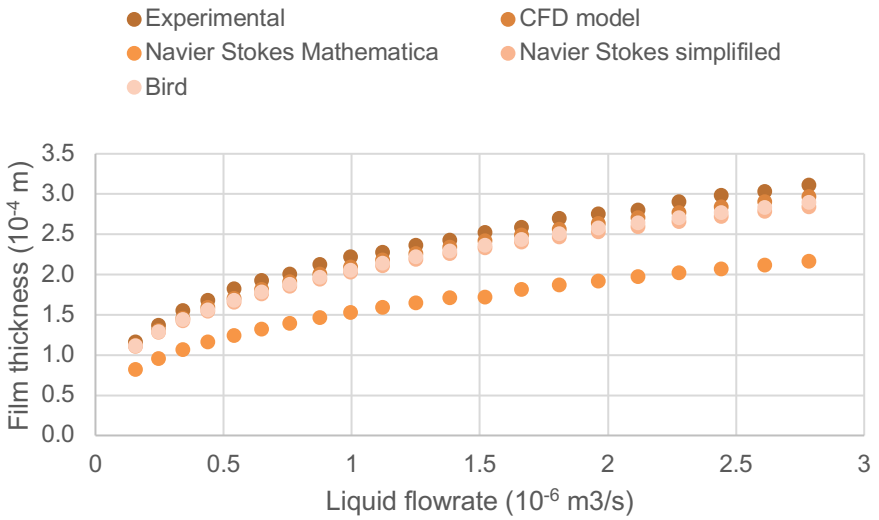

Figure 11. Influence of liquid flowrate on the film thickness (water)

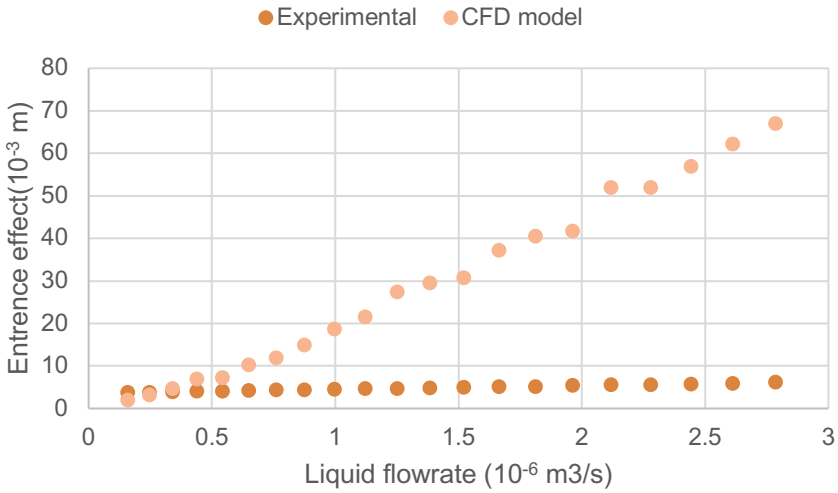

Figure 10. Influence of liquid flowrate on entrance effect (water)

To sum up, water film thickness and entrance region length increase with the flow rate. Besides, CFD model, Navier-Stokes simplified model and Bird model film thickness results are similar to experimental data but CFD model entrance region results differ from experimental data.

4.2.2.40% WATER-SUGAR SOLUTION

In this section, the same influence that in the previous section is studied but, in this case, using a 40% water-sugar solution. The Figure 12 shows how the liquid film thickness results obtained by the different models and experimental data change with the flow rate and the Figure 13 shows the influence of the liquid flowrate on the CFD and experimental entrance region.

The results show that the increasing tendency of the liquid film thickness and the entrance region length by the flowrate is also present in this liquid. In this liquid the CFD model, the Bird model and the Navier-Stokes simplified model film thickness results are similar but experimental data differ a little from them (Figure 12). Another change is that the different models results (except form Navier Stokes Mathematica model) are more similar to experimental data in higher flowrates. Moreover, Navier-Stokes Mathematica model is the most similar to experimental data at lowest liquids flowrates.

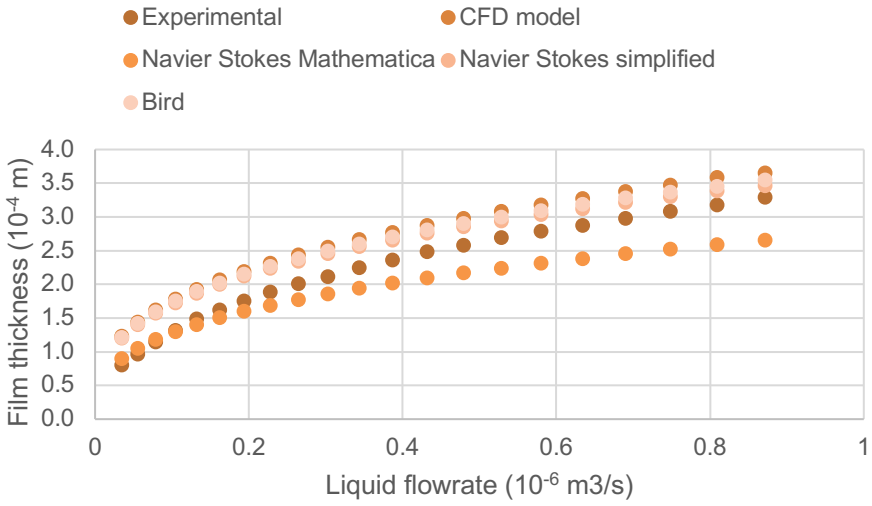

Figure 12 Influence of liquid flowrate on the film thickness (40% wt-sugar)

The entrance effect length results obtained with CFD simulation and experimentally are different but less than in distillate water case (Figure 13). Nevertheless, both of them increase with the flow rate.

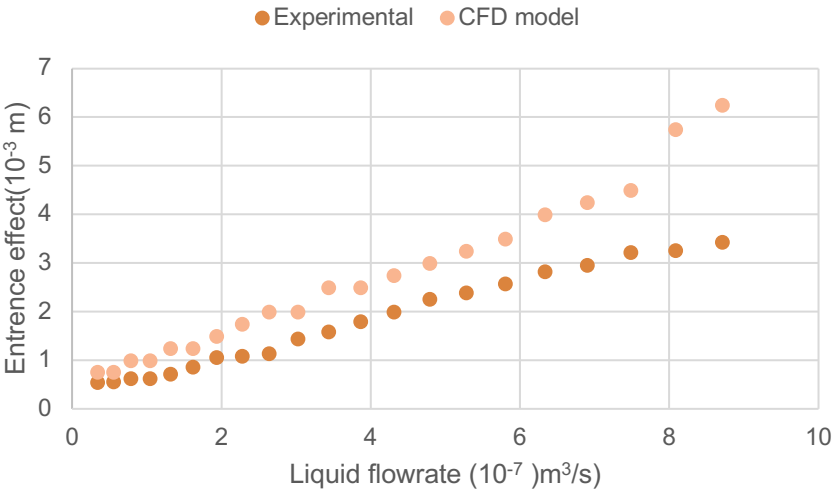

Figure 13. Influence of liquid flowrate on entrance effect (40% wt-sugar)

Summarizing, 40% water-MEA solution film thickness and entrance region length increase with the liquid flow rate as the water do but, in this case, CFD model, Navier-Stokes simplified model and Bird model film thickness results are bit different of experimental data. Maybe the differences between models and experimental data is because the viscosity of the liquid. In spite of this, experimental data and CFD model entrance region results are more similar.

4.2.3. 30% WATER-MEA SIMULATION

Finally, the same influence that in the other sections is studied using a 30% water-MEA solution. The influence of flowrate on the liquid film thickness result of the models and the experimental data is showed on Figure 14 and its influence on the entrance effect length results of the CFD model and experimental date is show in Figure 15 .

In this case the film thickness results (Figure 14) show that there is not a big different between models and experimental data as the same way that in water results, except form the case of the Navier-Stokes Mathematica model. But in this case, they also reveal that experimental data and models' results are more similar in intermediate flow. Besides, they show the film thickness increase with the flow rate as the same way than in the other liquids do.

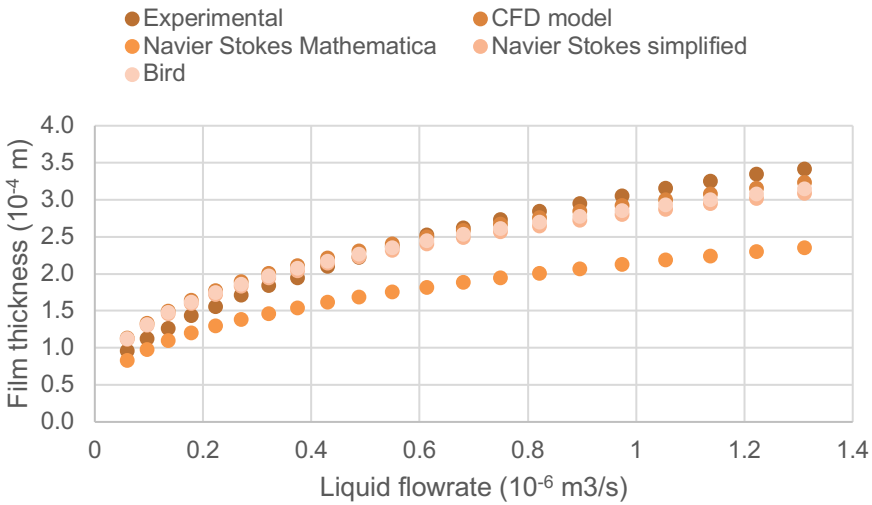

Figure 14. Influence of liquid flowrate on film thickness (30% wt-MEA)

In the other hand, the entrance effect length (Figure 15) also increase with the flowrate. Therefore, the CFD model results has an importance deviation form experimental date but less than using water.

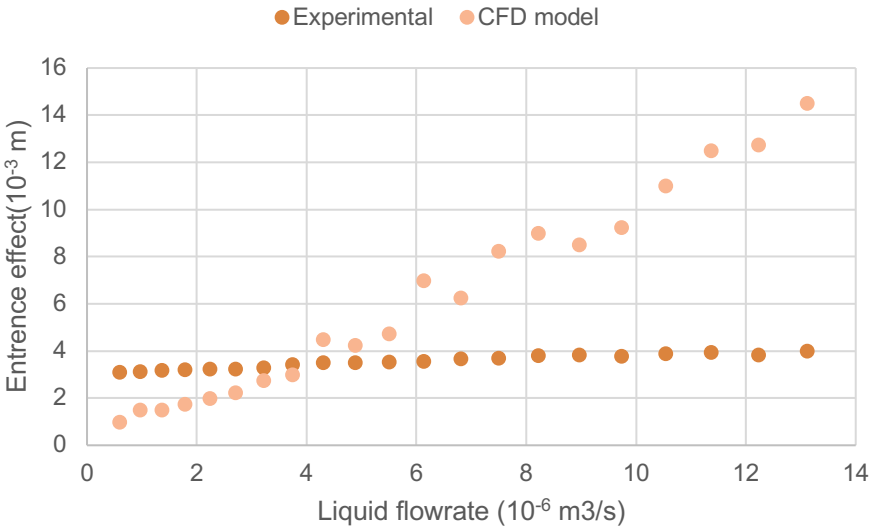

Figure 15. Influence of liquid flowrate on entrance effect (30% wt-MEA

In conclusion, according all the models and experimental data the liquid film thickness and the entrance region length increase with the flowrate independently of the liquid. However, the models are more or less similar to experimental data depending on which liquid is used. in the case of film thickness the differences are not significant at all.

Besides the CFD model, as the comparison of it with the experimental data show, can be used to predict the film thickness but not to predict the entrance region length. Nevertheless, the caparisons reveal that the liquids proprieties influence on the validity of the CFD model to predict the liquid film thickness. Specifically, the viscosity influences this adjustment because the three liquids have a similar density but a different the viscosity and because these are the only liquid properties that the CFD consider. In the flowing sections more detailed study of the CFD model is done.

4.3. CFD HYDRODYNAMIC ENTRY LENGTH

During the previous section some CFD simulations have been done to check the influence of the flowrate on the entrance region length. Moreover, the CFD results are compared with experimental data. These comparisons reflect that CFD model does not predict correctly the entrance region effect length. For this reason, a more detailed comparison of dimensionless entrance region lengths obtained with the CFD model and experimentally is done and the influence of Reynolds number on the CFD results is checked.

4.3.1. MODEL VALIDIY

The simulations done show that the hydrodynamic entry length calculated by CFD model is different form experimental value, it is why more detailed study of it is done. This length could be expressed as a dimensionless number. In Figure 16 a comparison of hydrodynamics entry length dimensionless values obtained experimentally and by simulations is shown. The figure reflects that CFD model is not a good model to predict the hydrodynamics entry length specially in liquid that have a lowest viscosity (distillate water and 30% water-MEA solution) and it is results are better in the liquid which has a higher viscosity.

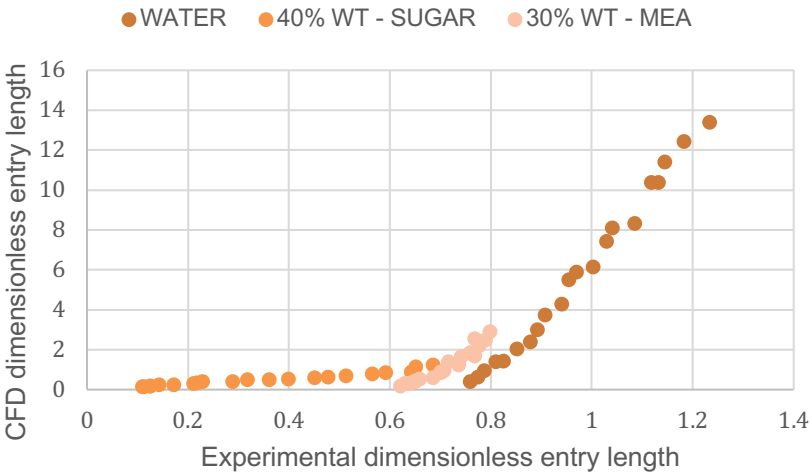

Figure 16. Dimensionless hydrodynamic entry length comparative

4.3.2. INFLUENCE OF REYNOLDS NUMBER

Many investigations are done to stablish a model to predict the hydrodynamics effect. In spite of this, they are not good enough to do a rigorous prediction and they so complicated. However, some experimental studies show that there is a relationship between the dimensionless hydrodynamic entry length and Reynolds Number (Eq.51). This relationship is related with the viscosity and the surface tension of the liquid and it indicate that the dimensionless entry length increases by Reynolds number. This is a lineal correlation which slope depended on the viscosity and the surface tension (Eq.52).

$$\lambda = a \cdot Re + b \quad (51)$$

$$a = 0{,}0008 \cdot e^{8197 \cdot \mu \cdot \sigma} \quad (52)$$

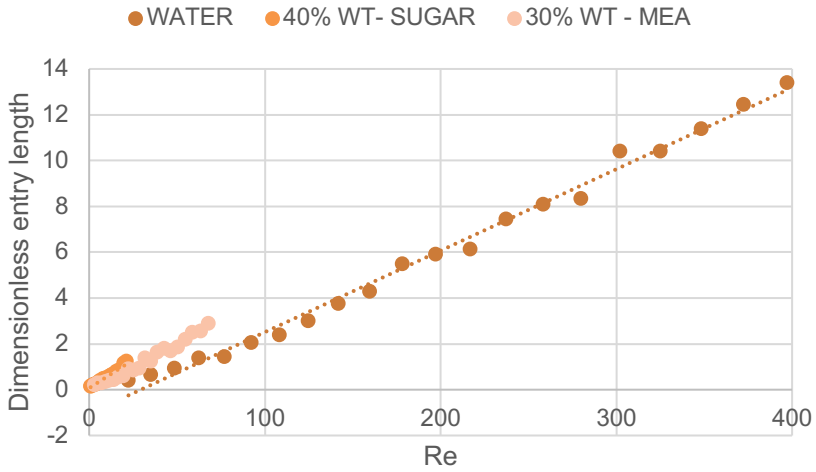

Figure 17. Influence of Reynolds Number on CFD dimensionless hydrodynamic entry length

Figure 17 shows the influence of Reynolds number on the entrance region lengths obtained using the CFD model to simulate the liquid film flow of the three liquids. The figure shows that the CFD dimensionless entry length increase lineally with Reynolds number as experimental studies.

This model does not consider the surface tension of the liquid. So maybe this reason and the initial film thickness assumed in the model are the reasons why CFD model is not adjusted to experimental data.

The results of lineal regression of the three liquids are on Table 3, Table 4 and Table 5. These results show that all liquids are well adjusted to a lineal equation. Moreover, they show that the intercept values of the lineal correlations are very different depending on the liquid which have been simulated but all slop values are of the same magnitude order.

Table 3. Distillate water lineal regression

a	0.0356
b	30.5815
R^2	0.9962

Table 4. 40% water-sugar solution lineal regression

a	0.0495
b	-1.0558
R^2	0.9865

Table 5. 30% water-MEA solution lineal regression

a	0.0412
b	2.0665
R^2	0.9900

Summarizing, the CFD model is not valid to predict the entrance region length. It may be because the model not consider the liquid surface tension and it uses an initial assuming film thickness. Nevertheless, their results are lineally influenced with Reynolds number such as experimental studies reflected.

4.4. INFLUENCE OF LIQUID ON CFD MODEL

The comparison of the CFD model film thickness with experimental data values shows that the CFD model adjusts better or worse to experimental data depending on the liquid. For this reason, a flowrate is fixed to show how the liquid film thickness changes along the tube depending on the liquid. By this way how viscosity value on affect the film thickness is also checked. Two flow rates have been fixed:

- Large feed flow rate of 50 millilitre per minute
- Low feed flow rate of 25 millilitre per minute

4.4.1. LARGE FEED FLOWRATE

First the large feed flow of 50 millilitre per minute have been fixed, the result of the CFD simulation are in Figure 18 and Figure 19. The first one shows the evolution of film thickness along the tube using different liquids. These result shows that the thicknesses increase with the viscosity value.

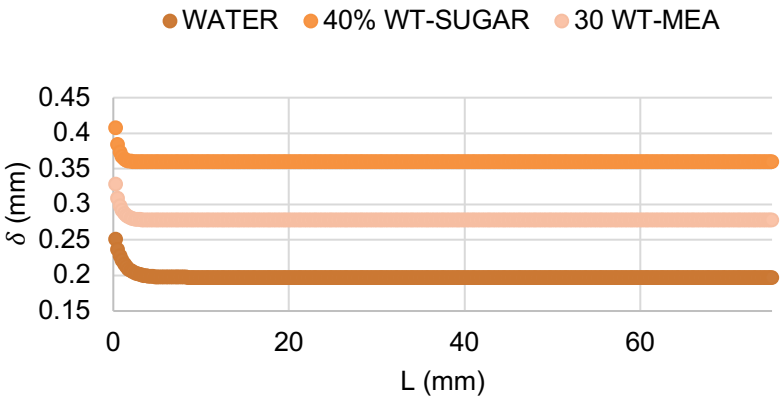

Figure 18. Evolution of liquid film thickness along the vertical tube (Q = 50 mL/min)

By the other hand, the other figure shows the upper part of the tube results. These simulations reflect that the film thickness stabilizes faster in the more viscous liquid (40% water-sugar solution). Hence, the entry region decreases with the viscosity.

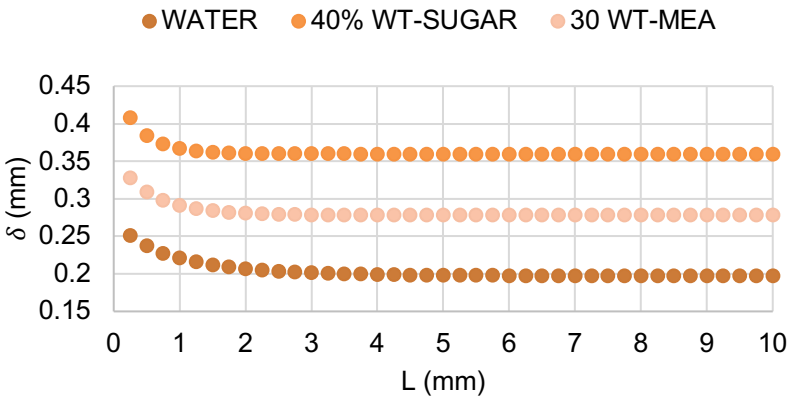

Figure 19 Evolution of liquid film thickness along the vertical tube on upper part (Q = 50 mL/min)

4.4.2. LOW FEED FLOWRATE

In this section the low feed flow of 25 millilitre per minute have been fixed, the result of the simulation are in Figure 20 and Figure 21.

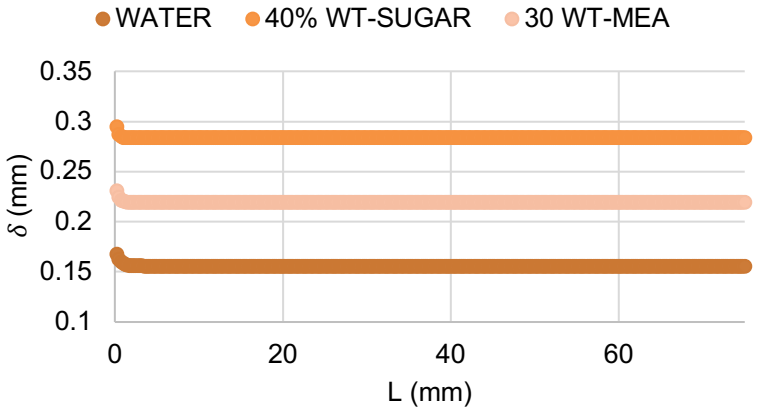

Figure 20. Evolution of liquid film thickness along the vertical tube (Q = 25 mL/min)

The first figure shows the evolution of film thickness along the tube using different liquids. These result shows that the thicknesses increase with the viscosity value, as the same way that it does using the large flow rate.

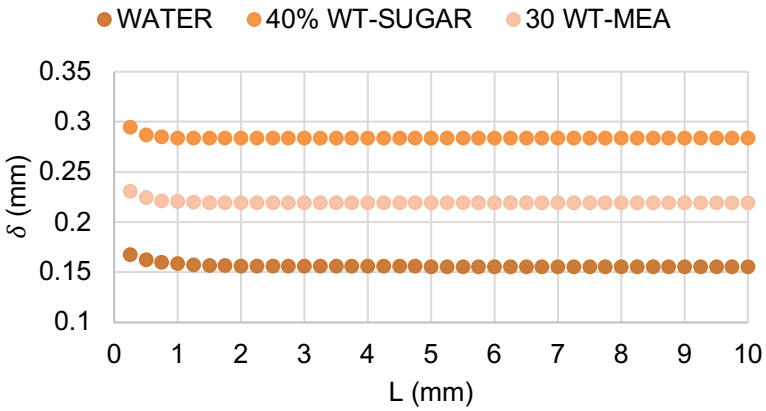

Figure 21. Evolution of liquid film thickness along the vertical tube on upper part (Q = 25 mL/min)

By the other hand, the other one shows the upper part of the tube results. These simulations reflect that the film thickness stabilizes faster in the more viscous liquid (40% water-sugar solution), as the same way that it does using the large flow rate. Therefore, the entry region decreases with the viscosity.

In conclusion the viscosity affects to the liquid film thickness obtained with the CFD model simulations. It flows a tendency of increasing with the liquid viscosity regardless of feed flowrate.

4.5. LIQUID FILM FLOW SKETCH

Sometimes is not easy to imagine how the liquid film flows along a tube, as a way to help four sketches of how liquid films flow along this tube are done. Specifically, they are done using the results of CFD simulation of the previous section.

Figure 22 and Figure 23 show a sketch of the three liquid film flow along the vertical tube using a large flowrate, but the first one is of the tube section and length and the second is of the upper left section. By the other hand, Figure 24 and Figure 25 show the same sketches but of the low feed flowrate results.

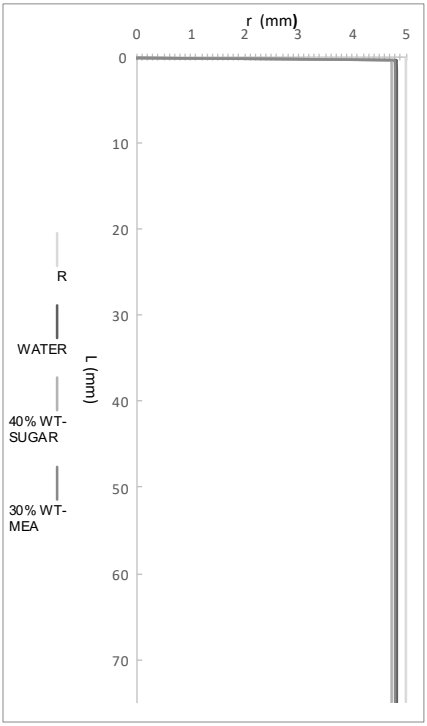

Figure 22. Sketch of liquid film flow along the vertical tub (Q = 50 mL/min)

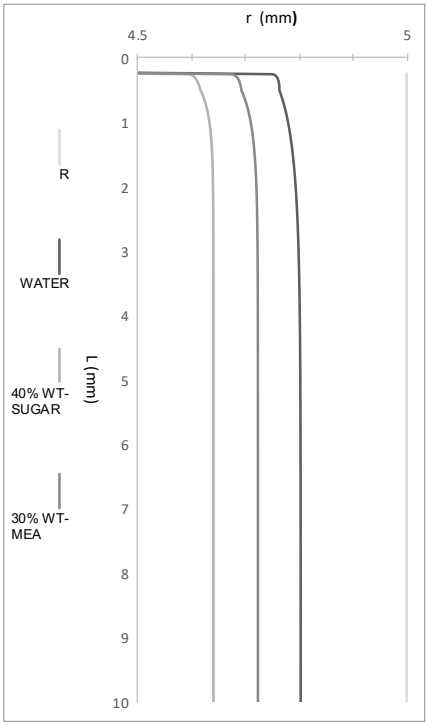

Figure 23. Expanded Sketch of liquid film flow along the vertical tub (Q = 50 mL/min)

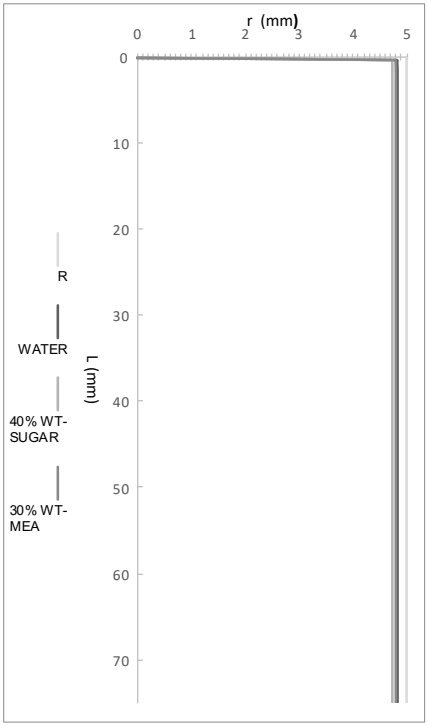

Figure 24. Sketch of liquid film flow along the vertical tub (Q = 25 mL/min)

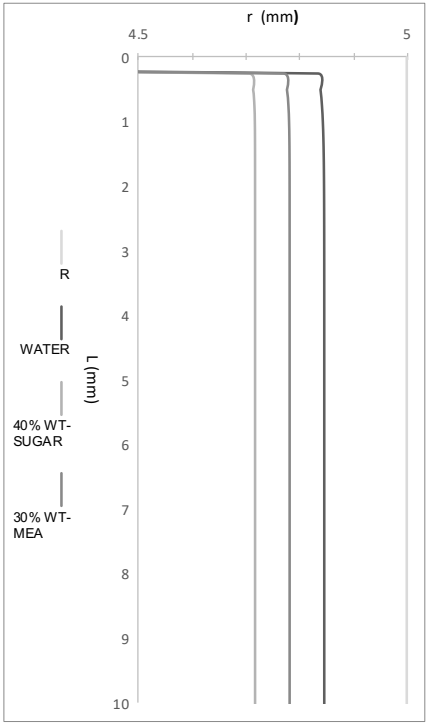

Figure 25. Expanded Sketch of liquid film flow along the vertical tub (Q = 25 mL/min)

Concluding, these sketches help us to imagine how the liquid flows along the tube. Comparing them the tendencies of the increases of the liquid film thickness with the flow rate and the viscosity are revalidated. Besides they show a thinking notch on the entrance region that may be the reason of the discrepancies between the CFD model and the experimental data.

5. CONCLUSIONS

The liquid film flow has been studied in this project because its importance on the actual chemical engineering processes. Specifically, a CFD model has been implemented to simulate the descending liquid film along a vertical tube and by this way reproducing an article published by Hogxia Gao in the AIChE journal on 2018. According on the comparison of it with three more models (Navier-Stokes Mathematica model, Navier-Stokes simplified model and Bird model) and experimental data published in the article, the CFD model is valid to predict the film thickness. By the other hand, despite following experimental tendency of increasing with the Reynolds number, the CFD model cannot be used to predict the entrance region length.

Furthermore, the computational results depend on the quality of meshing, but a high number of intervals on the meshing increase significantly the computational time. These results show that film thickness and hydrodynamics entrance length increase with the liquid flow rate. The similarity of the predicted parameters with experimental data depended on the liquid (distilled water / 40% water-sugar solution / 30% MEA-water solution).Besides, a comparison between the different liquids film flows reflects that numerical film thickness increases with liquid viscosity, but it stabilizes using less longitude of the tube meaning that the entrance region is smaller.

In conclusion, CFD model proposed based on Transports Phenomena subject is a good way to predict the film thickness of a descendent liquid film along a vertical tube according the comparison done using experimental data, Navier-Stokes simplified model and Bird model.

REFERENCES AND NOTES

- Álvarez E, G_omez-D_ıaz D, La Rubia MD, Navaza JM. Densities and viscosities of aqueous ternary mixtures of 2-(methylamino) etanol and 2-(ethylamino) ethanol with diethanolamine, triethanolamine, N-methyldiethanolamine, or 2-amino-1-methyl-1-propanol from 298.15 to 323.15 K. J Chem Eng Data. 2006;51(3):955–962.
- Amundsen TG, Øi LE, Eimer DA. Density and viscosity of mono-ethanolamine1 water1 carbon dioxide from (25 to 80) C. J Chem Eng Data. 2009;54(11):3096–3100.
- Andersson HI, Ytrehus T. Falkner-Skan solution for gravity-driven film flow. *J Appl Mech.* 1985;52(4):783–786.
- Bird R, Stewart W, Lightfoot E. Transport Phenomena. New York: Wiley, 1960.
- Grossman G. Simultaneous heat and mass transfer in film absorption under laminar flow. Int J Heat Mass Transf. 1983;26(3):357–371.
- Hassan NA. Laminar flow along a vertical wall. J Appl Mech. 1967;34(3):535–537.
- Hogxia Gao, Xiao Lou, Dig Cui, Zhiwu Liang, Xiayi Hu, Ardi Hartono, Hallvard F.Svendsen) A study of film thickness and hydrodynamic entrance length in liquid laminar film flow along a vertical tube. AlChe. January 2018.
- Kapitza P, Kapitza S. Wave flow of thin viscous fluid layers. Zh Eksp Teor Fiz. 1948;18(3):3–28.
- Lawrence PS, Rao BN. Similarity solutions for laminar thin-film flow along a vertical wall. *J Phys D Appl Phys.* 1993;26(6):928.
- Llorens, J. Apunts de Fenòmens de Transport. Universitat de Barcelona. 2019
- Min JK, Park IS. Numerical study for laminar wavy motions of liquid film flow on vertical wall. Int J Heat Mass Transf. 2011;54(15): 3256–3266.
- Mora, X. (2008). Les equacions de Navier-Stokes. Un repte al determinisme newtonià. Butlletí de la Societat Catalana de Matemàtiques, 23, 53–120. doi: 10.2436/20.2002.01.12
- Murty NS, Sastri VMK. Accelerating laminar liquid film along an inclined wall. Chem Eng Sci. 1973;28(3):869–874.
- Nakoryakov V, Grigor'eva N. Combined heat and mass transfer during absorption in drops and films. J Eng Phys Thermophys. 1977;32(3):243–247.
- *Nusselt W. Die Oberflachenkondesation des Wasserdamffes the surface condensation of water. Zetrschr Ver Deutch Ing. 1916; 60:541–546.*
- Portalski S. Studies of falling liquid film flow film thickness on a smooth vertical plate. Chem Eng Sci. 1963;18(12):787–804.
- Roy TR. On laminar thin-film flow along a vertical wall. *J Appl Mech*. 1984;51(3):691–692.
- Ruschak KJ, Weinstein SJ. Thin-Film flow at moderate Reynolds number. *J Fluids* Eng. 2000;122(4):774–778.

- Tekic´MN, Po_sarac D, Petrovic´D. Entrance region lengths of laminar falling films. *Chem Eng Sci.* 1984;39(1):165–167.
- Trela M. Minimum wetting rate for a decelerating liquid film*. Int J Heat Fluid Flow.* 1988;9(4):415–420.
- Vázquez G, Alvarez E, Navaza JM, Rendo R, Romero E. Surface tension of binary mixtures of water1 monoethanolamine and water1 2-amino-2-methyl-1-propanol and tertiary mixtures of thess amines with water from 25 C to 50 C. J Chem Eng Data. 1997; 42(1):57–59.

ACRONYMS

$\vec{\vec{\dot{\gamma}}}$: strain rate tensor, s^{-1}

Δr: radial position increment, -

Δr^*: dimensionless radial position increment, -

Δz^*: dimensionless axial position increment, -

c: velocity constant

D: experimental apparatus diameter, m

Eq.: equation γ

Fr: Froude Number, -

g: gravity acceleration, m/s^2

i: radial position, -

L: length, m

NN: last point of radius mesh, -

nr: radius intervals, -

nz: length intervals, -

Q: volumetric flowrate, m^3/s

Q*: dimensionless volumetric flowrate, -

r: radial position of cylinder, m

R: radius of cylinder, m

r*: dimensionless radial position, -

r1: internal radius, m

Re: Reynolds number, -

u: lineal velocity of liquid, m/s

u*: dimensionless lineal velocity of liquid, -

v: lineal velocity of liquid, m/s

W: circumference of cylinder in wetted wall column, m

z: axial position of cylinder, m

z*: dimensionless axial position, -

α: dimensionless film thickness, -

δ: film thickness, m

δ*: dimensionless film thickness, -

λ_E: hydrodynamic entrance length, m

μ: viscosity, kg/m·s

ρ: density, kg/m^3

τw: shear stress, N

ϕ: dimensionless radial position, -

APPENDICES

APPENDIX 1:

CFD MODEL PROGRAM

CFD MODEL

IMPORTANT: only dimensionless numbers are used in this program. So, it means that in spite of not using asterisk Δz, Δr, u, z, r and δ are dimensionless numbers.

In[•]:=
```
Quit[]
```
detén núcleo del sistema

SHPERICAL COORDINATES (Rr,Ttheta, Zz)

Out[•]=

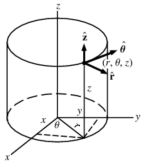

Liquid properties (ρ, μ), tube dimensions (R, L), and liquid flowrate (CV). All have to be expressed with international system units.

NUMERCIAL DATA

In[•]:=
```
g = 9.8;
ρ = 1010.6;
RR = 0.005;
μ = 0.00248;
CV = 3.57 / 10^6 × 60;
L = 0.075;
```

FLOW CIRCULATION

It is necessary to calculate the Reynolds number (reyn) and the Froude (Fr) number because they are included on the discretization equations. To do date the velocity (V) is obtained by volumetric flow expression.

In[•]:=
```
Print["CV = ", N[CV], " m^3/s"]
```
escribe valor numérico

```
V = CV / (π RR^2);
Print["V = ", V, " m/s"]
```
escribe

```
reyn = V RR ρ / μ; Fr = V / √(9.8 RR);
Print["Fr = ", Fr, "   Re = ", reyn]
```
escribe parte real

2 |

LENGTH DIVISION

```
tz = L/RR;
nz = 300;
Δz = Rationalize[tz / nz];
     |racionaliza
Print["Δz* = ", Δz]
|escribe
Print["Δz = ", Δz RR, " m"]
|escribe
Print["lenght intervals = ", nz]
|escribe
```

Space division is done along the length using 300 intervals

FILM THICKNESS INICIAL AND ASSUMING VALUE

```
δ[0] = 1;
Table[δ[z] = 0.01, {z, Δz, tz, Δz}];
|tabla
```

Initial film thickness

Assuming film thickness value along the tube

RADIUS DIVISION AND FUN

```
nr = 49;
NN = nr + 1;
Print[ "radius intervals = ", nr]
|escribe
Δr[z_] := δ[z]/nr
r[z_, i_] := (1 - δ[z]) + (i - 1) (δ[z]/nr);
coord := Table[{r[z, i], z}, {z, 0, tz, Δz}, {i, 1, NN}];
         |tabla
MatrixForm[coord];
|forma de matriz
```

Radius increment is defined using the assuming film thickness value

This table shows the meshing, along radial and axial directions.

INITIAL CONDITION

```
In[•]:= initialCond1 = Table[u_i[0] = 1, {i, 1, NN - 1}];
                       |tabla
```

BOUNDARY CONDITIONS

```
In[•]:= boundaryCond1 = Table[u_NN[z] = 0, {z, 0, tz, Δz}];
                        |tabla
```

Type one boundary condition is defiend.

| 3

DISCRETIZATION

In[•]:=

```
AE[z_, i_] := (r[z, i] + r[z, i + 1])/(2 reyn Δr[z]);
AW[z_, i_] := (r[z, i] + r[z, i - 1])/(2 reyn Δr[z]);
eq[i_] := ((r[z, i + 1]^2 - r[z, i - 1]^2) u_i[z - Δz])/(4 Δz) + AW[z, i] + AE[z, i]) u_i[z] ==
    AW[z, i] u_(i-1)[z] + AE[z, i] u_(i+1)[z] +
      ((r[z, i + 1]^2 - r[z, i - 1]^2) u_i[z - Δz]^2)/(4 Δz) + (r[z, i + 1]^2 - r[z, i - 1]^2)/(4 Fr^2);
i = 2;
eq[2] =
   ((r[z, i + 1]^2 - r[z, i - 1]^2) u_i[z - Δz])/(4 Δz) + 0 + AE[z, i]) u_i[z] == 0 + AE[z, i] u_(i+1)[z] +
     ((r[z, i + 1]^2 - r[z, i - 1]^2) u_i[z - Δz]^2)/(4 Δz) + (r[z, i + 1]^2 - r[z, i - 1]^2)/(4 Fr^2);
eq[1] := u_1[z] == u_2[z];
eqns := Flatten[Join[{eq[1]}, {eq[2]}, Table[eq[i], {i, 3, NN - 1}]]];
        aplana   junta                  tabla
MatrixForm[eqns];
forma de matriz
```

General equation is defined using Mathematica 12.0 code

Type two boundary condition

Equations applied along the radius

To obtain the velocity profile and the film thickness an interactive process is needed. This process using Mathematica 12.0 include the function Do [] to solve the velocity profile along axial direction and a While [] to obtain the film thickness

4 |

SOLUTION

n is the counter to solve the equations along the length

```
In[•]:= n = 0;
Do[n = n + 1;
 [repite
  z = n Δz; unknown = Flatten[{Table[uᵢ[z], {i, 1, NN - 1}]}];
                      [aplana  [tabla
  solution = NSolve[eqns, unknown][[1]];
             [resolvedor numérico
  Q = Σ_{i=2}^{NN} ((r[z, i])^2 - (r[z, i - 1])^2) (uᵢ[z] + uᵢ₋₁[z])/2 /. solution;
  While[Abs[1 - Q]/1 > 10^-12, δ[z] = √(1/Q) δ[z];
  [mientras
    solution = NSolve[eqns, unknown][[1]];
               [resolvedor numérico
    Q = Σ_{i=2}^{NN} ((r[z, i])^2 - (r[z, i - 1])^2) (uᵢ[z] + uᵢ₋₁[z])/2 /. solution;]
   Print["δ[", z, "] = ", δ[z] RR 1000, " mm"];
   [escribe
  Table[uᵢ[z] = uᵢ[z] /. solution, {i, 1, NN}];
  [tabla
  , {nz}]
result = Transpose[Table[uᵢ[z], {i, 1, NN}, {z, 0, tz, Δz}]];
          [transposición  [tabla
```

Numerical solver to obtain velocity profile along radius

New assuming dimensionless thickness

Volumetric flow conservation

Film thickness

Velocity profile along radial and axial direction

```
In[•]:= VelocityField = Table[{((1 - δ[j]) + (i - 1) δ[j]/nr) RR, -result[[j/Δz + 1, i]], V},
         [tabla
    {j, 0, tz, Δz}, {i, 1, NN}];
Show[Table[ListLinePlot[VelocityField[[i]]], {i, 2, nz + 1}],
     [tabla  [gráfico de línea de una lista
 GridLines → Automatic, PlotRange → Automatic]
             [automático  [rango de repr···  [automático
Print["Fr = ", Fr, "    Re = ", reyn]
                               [parte real
```

Velocity profile plot

APPENDIX 2:

NAVIER-STOKES MATHEMATICA PROGRAM

Film thickness (Navier Stokes)

```
In[•]:= Quit[]
        detén núcleo del sistema
```

BM

```
In[•]:= v = {0, 0, -vz[Rr]};
        Div[v, {Rr, Ttheta, Zz}, "Cylindrical"]
        divergencia
Out[•]= 0
```

Mass conservation equation expressed with Mathematica code

BQM

Momentum conservation equation expressed with Mathematica code

```
In[•]:= P = Press[0, 0, 0];
        grav = {0, 0, -g};
        Simplify[
        simplifica
         MatrixForm[-ρ (∂t v + v.Transpose[Grad[v, {Rr, Ttheta, Zz}, "Cylindrical"]]) -
         forma de matriz                transposición  gradiente
           Grad[P, {Rr, Ttheta, Zz}, "Cylindrical"] +
           gradiente
           μ (Laplacian[v, {Rr, Ttheta, Zz}, "Cylindrical"]) + ρ grav]]
              laplaciano
Out[•]//MatrixForm=
```

$$\begin{pmatrix} 0 \\ 0 \\ -\frac{g\,Rr\,\rho + \mu\,vz'[Rr] + Rr\,\mu\,vz''[Rr]}{Rr} \end{pmatrix}$$

Differential equation used to predict the velocity profile

DIFFERENTIAL EQUATION RESOLUTION

```
In[•]:= solution = DSolve[-(g Rr ρ + μ vz'[Rr] + Rr μ vz''[Rr])/Rr == 0, vz, Rr];
        resolvedor diferencial

        vz1[Rr_] = Simplify[(vz[Rr] /. solution)][[1]]
        simplifica
```

$$\text{Out}[\bullet]= -\frac{g\,Rr^2\,\rho}{4\,\mu} + c_2 + c_1\,\text{Log}[Rr]$$

Solution of differential equation

BOUNDARY CONDITIONS

1. v[R]=0

```
In[•]:= vz2[Rr_] = Simplify[vz1[Rr] /. Solve[vz1[R] == 0, {C[2]}][[1]]];
        simplifica                  resuelve          constante
        Print["vz = ", vz2[Rr]]
        escribe
```

$$vz = \frac{g\left(R^2 - Rr^2\right)\rho}{4\,\mu} - c_1\,\text{Log}[R] + c_1\,\text{Log}[Rr]$$

2. From the shear stress (calculed form the velocity equation and the force balance)

Boundary conditions are needed to obtain velocity profile. These are used to determined constants which are one the solution of the differential equation

2 | *NS PROGRMAE.nb*

Newton's law expressed with Mathematica code

```
In[•]:= v1 = {0, 0, vz1[Rr]};
        stress[Rr_] =
          Simplify[-μ (Transpose[Grad[v1, {Rr, Ttheta, Zz}, "Cylindrical"]] +
          [simplifica  [transposición  [gradiente
               Grad[v1, {Rr, Ttheta, Zz}, "Cylindrical"])];
                [gradiente
        MatrixForm[stress[Rr]]
        [forma de matriz
```

Out[•]//MatrixForm=

$$\begin{pmatrix} 0 & 0 & \frac{g\,Rr\,\rho}{2} - \frac{\mu\,c_1}{Rr} \\ 0 & 0 & 0 \\ \frac{g\,Rr\,\rho}{2} - \frac{\mu\,c_1}{Rr} & 0 & 0 \end{pmatrix}$$

Stress expression of the liquid descendent film

```
In[•]:= τws = (τw /. Solve[ρ g L π (r1^2 - R^2) + τw 2 π r1 L == 0, τw])[[1]];
              [resuelve
        Print[" Shear stress  = ", τws]
        [escribe
```

Shear stress = $\frac{g\left(R^2 - r1^2\right)\rho}{2\,r1}$

Force balance

```
In[•]:= vz3[Rr_] = Simplify[vz2[Rr] /. Solve[{stress[r1][[1, 3]] == τws}, {C[1]}][[1]];
                   [simplifica          [resuelve                        [constante
        Print["vz = ", vz3[Rr]]
        [escribe
```

vz = $\frac{g\rho\left(R^2 - Rr^2 + 2\left(R^2 - 2\,r1^2\right)\text{Log}[R] - 2\left(R^2 - 2\,r1^2\right)\text{Log}[Rr]\right)}{4\,\mu}$

Velocity profile

```
In[•]:=
```

FILM THICKNESS

```
In[•]:= μ = 0.0008899;
        L = 0.075;
        g = 9.8;
        R = 0.005;
        ρ = 997.056;
```

Mathematica cannot obtain the liquid flowrate expression using symbolical integration for this reason a numerical integration is done. To do that liquid proprieties and tube dimension are needed, these are expressed with international system units.

```
In[•]:=
```

Numerical integration

GRAPHICALLY

```
In[•]:= Plot[∫_r1^R vz3[Rr] 2 π 60 × 10^6 Rr dRr, {r1, 0, R}, GridLines → Automatic,
          representación gráfica                                parrilla de líneas automático
        PlotRange → {{0, R}, {9, 170}}, AxesLabel → {"R[m]", "Q [mL/min]"}]
                                                    etiqueta de ejes
```

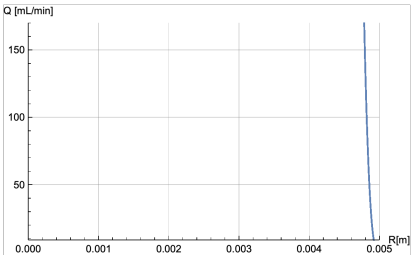

Out[•]=

Flowrate plot

Graphically the value of r1 is detarmined by the liquid flowrrate

NUMERICAALLY (INTERPOLATION)

1

This table express how the flowrate changes with different r1 values

```
In[•]:= CV = 9.41 / (60 × 10^6);

llista = Table[{N[∫_r1^R vz3[Rr] 2 π Rr dRr], r1}, {r1, 0.0045, 0.005, 0.00001}];
          tabla   valor numérico

r1 = Interpolation[llista][CV];
     interpolación

Print["r1 = ", r1 1000, " mm "]
escribe

Print["film thickness = ", (R - r1) 1000, " mm "]
escribe
```

To obtain the film thickness in every flowrate an interpolation is done. With the interpolation the r1 value is determined

```
r1 = 4.91786 mm

film thickness = 0.0821366 mm
```

APPENDIX 3:

INFLUENCE OF FLOWRATE SIMULATION RESULTS

Table 1 Experimental data (water)

No.	Re	δ(mm)	λ_E(mm)
1	22.4	0.1161	3.79
2	35.1	0.1366	3.87
3	48.5	0.1547	3.93
4	62.5	0.1675	4.05
5	77.2	0.1820	4.12
6	92.4	0.1926	4.26
7	108.3	0.2006	4.39
8	124.9	0.2127	4.46
9	142.0	0.2219	4.54
10	159.8	0.2278	4.70
11	178.3	0.2360	4.77
12	197.3	0.2426	4.85
13	217.0	0.2524	5.01
14	237.3	0.2587	5.14
15	258.3	0.2698	5.20
16	279.9	0.2750	5.43
17	302.1	0.2801	5.59
18	324.9	0.2901	5.66
19	348.4	0.2979	5.72
22	372.5	0.3034	5.91
21	397.3	0.3111	6.16

Table 2. CFD model results (water)

No.	Q(mL/min)	δ(mm)	λ_E(mm)
1	9.41	0.1123	2.00
2	14.77	0.1307	3.25
3	20.40	0.1457	4.75
4	26.30	0.1587	7.00
5	32.45	0.1704	7.25
6	38.88	0.1811	10.25
7	45.57	0.1909	12.00
8	52.52	0.2004	15.00
9	59.74	0.2093	18.75
10	67.23	0.2179	21.50
11	74.98	0.2261	27.50
12	83.00	0.2340	29.50
13	91.28	0.2417	30.75
14	99.83	0.2491	37.25
15	108.64	0.2564	40.50
16	117.72	0.2630	41.75
17	127.06	0.2704	52.00
18	136.67	0.2771	52.00
19	146.54	0.2838	57.00
22	156.68	0.2903	62.25
21	167.08	0.2967	67.00

Table 3. Navier-Stokes Mathematica model results (water)

No.	Q(mL/min)	δ(mm)
1	9.41	0.0821
2	14.77	0.0956
3	20.40	0.1065
4	26.30	0.1159
5	32.45	0.1244
6	38.88	0.1322
7	45.57	0.1394
8	52.52	0.1462
9	59.74	0.1527
10	67.23	0.1589
11	74.98	0.1649

No.	Q(mL/min)	δ(mm)
12	83.00	0.1706
13	91.28	0.1714
14	99.83	0.1815
15	108.64	0.1868
16	117.72	0.1919
17	127.06	0.1969
18	136.67	0.2018
19	146.54	0.2066
22	156.68	0.2114
21	167.08	0.2160

Table 4. Experimental data (40% sugar-water solution)

No.	Re	δ(mm)	λ_E(mm)
1	0.8	0.0799	0.55
2	1.4	0.0959	0.56
3	1.9	0.1139	0.62
4	2.5	0.1317	0.62
5	3.2	0.1482	0.71
6	3.9	0.1618	0.86
7	4.7	0.1749	1.06
8	5.5	0.1881	1.09
9	6.4	0.2006	1.14
10	7.4	0.2109	1.44
11	8.4	0.2241	1.59

No.	Re	δ(mm)	λ_E(mm)
12	9.4	0.2355	1.80
13	10.5	0.2479	2.00
14	11.7	0.2573	2.25
15	12.9	0.2695	2.39
16	14.1	0.2790	2.57
17	15.4	0.2872	2.82
18	16.8	0.2972	2.96
19	18.2	0.3079	3.21
22	19.7	0.3179	3.26
21	21.2	0.3285	3.42

Table 5. CFD model results (40% sugar-water solution)

No.	Q(mL/min)	δ(mm)	λ_E(mm)	No.	Q(mL/min)	δ(mm)	λ_E(mm)
1	2.08	0.1226	0.75	12	23.21	0.2768	2.50
2	3.34	0.1437	0.75	13	25.91	0.2873	2.75
3	4.74	0.1617	1.00	14	28.75	0.2977	3.00
4	6.27	0.1777	1.00	15	31.72	0.3078	3.25
5	7.92	0.1923	1.25	16	34.82	0.3177	3.50
6	9.71	0.2060	1.25	17	38.05	0.3275	4.00
7	11.63	0.2190	1.50	18	41.42	0.3371	4.25
8	13.69	0.2313	1.75	19	44.91	0.3466	4.50
9	15.87	0.2433	2.00	22	48.54	0.3588	5.75
10	18.18	0.2547	2.00	21	52.29	0.3651	6.25
11	20.63	0.2659	2.50				

Table 6. Navier-Stokes Mathematica model results (40% sugar-water solution)

No.	Q(mL/min)	δ(mm)	No.	Q(mL/min)	δ(mm)
1	2.08	0.0896	12	23.21	0.2016
2	3.34	0.1050	13	25.91	0.2092
3	4.74	0.1181	14	28.75	0.2167
4	6.27	0.1297	15	31.72	0.2240
5	7.92	0.1403	16	34.82	0.2312
6	9.71	0.1503	17	38.05	0.2382
7	11.63	0.1597	18	41.42	0.2452
8	13.69	0.1687	19	44.91	0.2520
9	15.87	0.1773	22	48.54	0.2587
10	18.18	0.1856	21	52.29	0.2653
11	20.63	0.1937			

Table 7. Experimental data (30% sugar-MEA solution)

No.	Re	δ(mm)	λ_E(mm)
1	3.09	0.0960	4.14
2	5.00	0.1125	4.20
3	7.05	0.1263	4.24
4	9.24	0.1435	4.28
5	11.57	0.1562	4.34
6	14.04	0.1718	4.39
7	16.65	0.1846	4.57
8	19.41	0.1952	4.67
9	22.30	0.2105	4.67
10	25.33	0.2223	4.71
11	28.51	0.2376	4.77
12	31.82	0.2529	4.91
13	35.28	0.2626	4.95
14	38.88	0.2739	5.08
15	42.62	0.2852	5.12
16	46.50	0.2954	5.06
17	50.52	0.3060	5.18
18	54.68	0.3161	5.26
19	58.98	0.3255	5.12
22	63.42	0.3346	5.12
21	68.01	0.3418	5.32

Table 8. CFD model results (30% sugar-MEA solution)

No.	Q(mL/min)	δ(mm)	λ_E(mm)
1	3.57	0.1139	1.33
2	5.78	0.1339	2.00
3	8.15	0.1504	2.00
4	10.68	0.1647	2.33
5	13.38	0.1777	2.67
6	16.24	0.1897	3.00
7	19.26	0.2010	3.67
8	22.44	0.2116	4.00
9	25.79	0.2218	6.00
10	29.30	0.2316	5.67
11	32.97	0.2411	6.33
12	36.80	0.2502	9.33
13	40.80	0.2592	8.33
14	44.96	0.2678	11.00
15	49.28	0.2763	12.00
16	53.77	0.2846	11.33
17	58.42	0.2928	12.33
18	63.23	0.3008	14.67
19	68.20	0.3086	16.67
22	73.34	0.3164	17.00
21	78.64	0.3240	19.33

Table 9. Navier-Stokes Mathematica model results (30% sugar-MEA solution)

No.	Q(mL/min)	δ(mm)
1	3.57	0.0833
2	5.78	0.0979
3	8.15	0.1098
4	10.68	0.1203
5	13.38	0.1297
6	16.24	0.1385
7	19.26	0.1466
8	22.44	0.1544
9	25.79	0.1618
10	29.30	0.1689
11	32.97	0.1757

No.	Q(mL/min)	δ(mm)
12	36.80	0.1824
13	40.80	0.1888
14	44.96	0.1951
15	49.28	0.2012
16	53.77	0.2073
17	58.42	0.2131
18	63.23	0.2189
19	68.20	0.2246
22	73.34	0.2302
21	78.64	0.2357